Inorg. Chem. **2003**, *42*, 3445–3453

Highly Sensitive Luminescent Metal-Complex Receptors for Anions through Charge-Assisted Amide Hydrogen Bonding

Shih-Sheng Sun, Alistair J. Lees,* and Peter Y. Zavalij

Institute for Materials Research and Department of Chemistry, State University of New York at Binghamton, Binghamton, New York 13902-6000

Received November 5, 2002

Two structurally simple and easily synthesized luminescent anion receptors featured with an amide-type anion binding site and rhenium(I) tricarbonyl pyridine signaling units have been developed, and they display outstanding sensitivity and selectivity toward a variety of anionic species. These complexes are highly emissive in solution. Upon anion binding, the emission intensity was significantly quenched. The sensitivities of these complexes are so high that the emission intensity can be effectively quenched by as much as 10% even in the presence of only 10^{-8} M cyanide or fluoride anions. The ability of formation of intramolecular hydrogen bonding between the amide protons and central pyridine is believed to be responsible for the observed high selectivity.

Introduction

Anions play very important roles in both biological systems and environmental chemistry. An important aspect of modern supramolecular chemistry is the utilization of hydrogen bonding in the development of receptors for the recognition of anions.[1] Although cation receptors have been studied for more than 4 decades, the development of anion receptors has received much less attention until the last 15 years or so. Compared to the relatively simple design principles for cation receptors (electrostatic interactions and sizes), there are more factors that can influence the effectiveness of the artificial anion receptors. Due to the fact that anions are larger than isoelectronic cations and, thus, have a smaller charge-to-radius ratio, electrostatic interactions are less effective for anions than their corresponding isoelectronic cations.[2] Solvation effects are also more prominent for anions than their isoelectronic cations, and this is an important factor to consider in designing artificial anion receptors. Hydroxylic solvents usually form strong hydrogen bonds with anions, and this will reduce the affinity of anions toward anion receptors. Hydrophobicity can also influence the selectivity of an anion receptor as hydrophobic anions tend to bind more tightly to the hydrophobic sites of the receptors. Therefore, to achieve the desired sensitive and selectivity, the combination of electrostatic attraction, hydrogen bonding, hydrophobic effects, and stacking effects all needs to be taken into consideration when designing artificial anionic hosts.[3]

The incorporation of luminescent chromophores into the receptor, which are sensitive to interactions between the host and guest molecules, has recently gained considerable attention due to their high sensitivity and low detection limit.[4,5] The appeal of sensors containing luminescence chromophores stems from the high sensitivity of luminescence detection compared to other spectroscopic methods. The binding of anionic species to the recognition sites leads to changes in certain properties of the receptors (such as luminescence, lifetime, etc.) that then serve as an indicator of guest association.

* To whom correspondence should be addressed. E-mail: alees@binghamton.edu. Fax: (+1)607-777-4478.

(1) (a) Beer, P. D.; Smith, D. K. *Prog. Inorg. Chem*. **1997**, *46*, 1. (b) Beer, P. D.; Gale, P. A. *Angew. Chem., Int. Ed*. **2001**, *40*, 486. (c) Fabbrizzi, L.; Licchell, M.; Rabaioli, G.; Taglietti, A. *Coord. Chem. Rev*. **2000**, *205*, 85.

(2) (a) Marcus, Y. *J. Chem. Soc., Faraday Trans. 1* **1991**, *87*, 2995. (b) Marcus, Y. *J. Chem. Soc., Faraday Trans. 1* **1987**, *83*, 339. (c) Marcus, Y. *J. Chem. Soc., Faraday Trans. 1* **1986**, *82*, 233.

(3) Bianchi, A., Bowman-James, K., García-España, E., Eds. *Supramolecular Chemistry of Anions*; Wiley-VCH Publishers: Toronto, Canada, 1997.

(4) (a) De Silva, A. P.; Gunaratne, H. Q.; Gunnlaugsson, N. T.; Huxley, A. J. M.; McCoy, C. P.; Rademacher, J. T.; Rice, T. E. *Chem. Rev*. **1997**, *97*, 1515. (b) Keefe, M. H.; Benkstein, K. D.; Hupp, J. T. *Coord. Chem. Rev*. **2000**, *205*, 201.

(5) Recent examples on transition-metal based luminescence sensing systems: (a) Charbonnière, L. J.; Ziessel, R.; Montalti, M.; Prodi, L.; Zaccheroni, N.; Boehme, C.; Wipff, G. *J. Am. Chem. Soc*. **2002**, *124*, 7779. (b) Anzenbacher, P., Jr.; Tyson, D. S.; Jursíková, K.; Castellano, F. N. *J. Am. Chem. Soc*. **2002**, *124*, 6232. (c) Watanabe, S.; Onogawa, O.; Komatsu, Y.; Yoshida, K. *J. Am. Chem. Soc*. **1998**, *120*, 229. (d) Fabbrizzi, L.; Faravelli, I.; Francese, G.; Licchelli, M.; Perotti, A.; Taglietti, A. *Chem. Commun*. **1998**, 971. (e) Parker, D.; Senanayake, P. K.; Williams, J. A. G. *J. Chem. Soc., Perkin. Trans. 2* **1998**, 2129. (f) Beer, P. D.; Szemes, F.; Balzani, V.; Sala, C. M.; Drew, M. G. B.; Dent, S. W.; Maestri, M. *J. Am. Chem. Soc*. **1997**, *119*, 11864.

10.1021/ic0206589 CCC: $25.00 © 2003 American Chemical Society
Published on Web 05/06/2003

Incorporating a transition metal into the framework of sensory systems offers several advantages over pure organic sensory systems. First, transition-metal complexes are usually positively charged or electron deficient in nature. This property leads to either the enhancement of the electrostatic interactions with negatively charged species or a higher probability of orbital overlap and, thus, stronger bonding interactions with anionic species. Second, transition-metal complexes typically possess precisely defined geometries. This characteristic is especially useful for enhancing the selectivity of certain shaped anions or inducing unusual structural changes upon binding to anions. Third, and perhaps the most appealing reason, is that transition-metal complexes possess a variety of unique functionalities such as redox activity, visible spectroscopic features (color), magnetism, luminescence, and catalytic ability. Incorporation of these functionality properties into sensory systems provides not only the improvement of sensor technology but also some other guest recognition based applications such as anion transport, drug delivery, and catalysis. Taking these possibilities into consideration, we designed a very simple and easily prepared luminescent metal-complex system integrated with an amide moiety functioning as a hydrogen-bonding site.[6] We have surprisingly found that this so-called tweezer or two-armed receptor exhibits exceptionally high sensitivity as well as selectivity toward a variety of anions.

Experimental Section

Materials and General Procedures. All starting chemicals were commercially available and used without further purification unless otherwise noted. The metal-complex precursors, (4,4′-*t*Bu_2bpy)Re$(CO)_3(CH_3CN)(PF_6)$ (4,4′-*t*Bu_2bpy is 4,4′-bis-*tert*-butyl-2,2′-bipyridine) and (6-Mebpy)Re$(CO)_3(CH_3CN)(PF_6)$ (6-Mebpy is 6-methyl-2,2′-bipyridine), were synthesized according to a published method.[7]

Synthesis. *N,N′*-Dipyridin-4-ylpyridine-2,6-dicarboxamide (1). To a 250-mL flask containing pyridine-2,6-dicarbonyl dichloride (1.00 g, 4.90 mmol) and 4-aminopyridine (0.926 g, 9.85 mmol) were successively added 100 mL of CH_2Cl_2 and 3 mL of NEt_3. The resulting mixture was stirred at room temperature for 24 h. The resulting white precipitate was collected on frit, washed with CH_2Cl_2 (50 mL × 3), and dried in a vacuum oven to afford 880 mg of white powder. Yield: 56%. ^{1}H NMR (300 MHz, acetone-d_6): 10.78 (s, 2 H, −N*H*), 8.55 (d, 4 H, $^3J_{H-H}$ = 6.4 Hz, H_α-py), 8.50 (d, 2 H, $^3J_{H-H}$ = 8.2 Hz, H_m-py), 8.37 (t, 1 H, $^3J_{H-H}$ = 8.5 Hz, H_p-py), 7.96 (d, 4 H, $^3J_{H-H}$ = 6.4 Hz, H_β-py). ^{13}C NMR (acetone-d_6): 163.2, 151.6, 149.8, 145.9, 141.1, 126.9, 115.2. EI-MS: *m*/*z* = 319.1 (calcd *m*/*z* = 319.1 for $[M]^+$). Anal. Calcd for $C_{17}H_{13}N_5O_2$: C, 63.94; H, 4.10; N, 21.93. Found: C, 63.66; H, 4.05; N, 21.68.

***N,N′*-Dipyridin-4-ylisophthalamide (2).** The same procedure of preparing ligand **1** was employed to synthesized **2**. Yield: 72%. ^{1}H NMR (300 MHz, DMSO-d_6): 10.35 (s, 2 H, −N*H*), 8.09 (s, 1 H, Ph-2), 8.04 (d, 4 H, $^3J_{H-H}$ = 5.9 Hz, H_α-py), 7.73 (d, 2 H, $^3J_{H-H}$ = 7.8 Hz, Ph-4,6), 7.35 (d, 4 H, $^3J_{H-H}$ = 6.2 Hz, H_β-py), 7.28 (t, 1 H, $^3J_{H-H}$ = 7.8 Hz, Ph-5). ^{13}C NMR (DMSO-d_6): 165.8, 150.3, 145.7, 134.5, 131.3, 128.8, 127.3, 114.0. EI-MS: *m*/*z* = 318.1 (calcd *m*/*z* = 318.1 for $[M]^+$). Anal. Calcd for $C_{18}H_{14}N_4O_2$: C, 67.91; H, 4.43; N, 17.60. Found: C, 67.83; H, 4.10; N, 17.89.

***N,N′*-Dipyridin-4-ylterephthalamide (3).** To a 500-mL flask containing terephthaloyl chloride (0.5 g, 2.46 mmol) and 4-aminopyridine (0.48 g, 5.20 mmol) were successively added 200 mL of CH_2Cl_2 and 3 mL of NEt_3. The resulting mixture was stirred at room temperature for 24 h. The resulting white precipitate was collected on frit, washed with water (50 mL × 2) and CH_2Cl_2 (50 mL × 2), and dried in a vacuum oven to afford 485 mg of white powder. Yield: 62%. ^{1}H NMR (300 MHz, DMSO-d_6): 10.75 (s, 2 H, −N*H*), 8.50 (d, 4 H, $^3J_{H-H}$ = 4.9 Hz, H_α-py), 8.11 (s, 4 H, Ph), 7.80 (d, 4 H, $^3J_{H-H}$ = 4.9 Hz, H_β-py). ^{13}C NMR (DMSO-d_6): 165.7, 150.3, 145.7, 137.1, 128.0, 114.1. EI-MS: *m*/*z* = 318.1 (calcd *m*/*z* = 318.1 for $[M]^+$). Anal. Calcd for $C_{18}H_{14}N_4O_2$: C, 67.91; H, 4.43; N, 17.60. Found: C, 67.58; H, 4.36; N, 17.81.

$[(4,4'\text{-}t\text{Bu}_2\text{bpy})\text{Re}(CO)_3]_2(\mu\text{-}1)(PF_6)_2$ (4). (4,4′-*t*Bu_2bpy)Re$(CO)_3(CH_3CN)(PF_6)$ (300 mg, 0.41 mmol) and ligand **1** (63 mg, 0.20 mmol) were placed in a 100-mL flask. To this flask was added 25 mL of THF, and the mixture was refluxed for 5 h. The solvent was evaporated under vacuum, and the residue was dissolved in 20 mL of CH_2Cl_2. Any insoluble solid was filtered off, and the filtrate was layered with 100 mL of pentane for 3 days. The resulting yellow crystalline solid was collected and dried in vacuo to afford 270 mg of yellowish powder. Yield: 81%. IR ($\nu_{C\equiv O}$, CH_2Cl_2): 2032, 1928. ^{1}H NMR (300 MHz, $CDCl_3$): 10.59 (s, 2 H, −N*H*), 8.91 (d, 4 H, $^3J_{H-H}$ = 5.9 Hz, $H_{6,6'}$-Bu_2bpy), 8.34 (d, 2 H, $^3J_{H-H}$ = 7.7 Hz, H_m-py), 8.28 (s, 4 H, $H_{3,3'}$-Bu_2bpy), 8.04 (t, 1 H, $^3J_{H-H}$ = 7.6 Hz, H_p-py), 7.93 (d, 4 H, $^3J_{H-H}$ = 6.4 Hz, H_α-py), 7.81 (d, 4 H, $^3J_{H-H}$ = 6.6 Hz, H_β-py), 7.67 (d, 4 H, $^3J_{H-H}$ = 7.1 Hz, $H_{5,5'}$-Bu_2bpy), 1.46 (s, 36 H, −C*H*$_3$). ^{13}C NMR ($CDCl_3$): 196.3, 192.0, 166.3, 162.7, 155.8, 152.6, 152.1, 148.0, 147.7, 139.7, 126.6, 126.4, 122.0, 117.1, 36.3, 30.3. ES-MS: *m*/*z* = 1540.2 (calcd *m*/*z* = 1541.6 for $[M - PF_6^-]^+$) and *m*/*z* = 698.6 (calcd *m*/*z* = 698.3 for $[M - 2PF_6^-]^{2+}$). Anal. Calcd for $C_{59}H_{61}N_9O_8Re_2P_2F_{12}$: C, 42.02; H, 3.65; N, 7.47. Found: C, 41.80; H, 3.62; N, 7.26.

$[(6\text{-Mebpy})\text{Re}(CO)_3]_2(\mu\text{-}1)(PF_6)_2$ (5). The same procedure for preparing **4** was employed to synthesize **5**. The purification was achieved by recrystallization from CH_3CN/ether to give the yellowish powder of **5**. Yield: 88%. IR ($\nu_{C\equiv O}$, CH_2Cl_2): 2035, 1933. ^{1}H NMR (300 MHz, acetone-d_6): 11.06 (s, 2 H, −N*H*), 9.46 (d, 2 H, $^3J_{H-H}$ = 5.4 Hz, $H_{6'}$-Mebpy), 8.61 (d, 2 H, $^3J_{H-H}$ = 8.0 Hz, $H_{3'}$-Mebpy), 8.47 (d, 2 H, $^3J_{H-H}$ = 8.1 Hz, H_3-Mebpy), 8.45−8.40 (m, 4 H, H_m-py, $H_{4'}$-Mebpy), 8.37 (t, 1 H, $^3J_{H-H}$ = 7.7 Hz, H_p-py), 8.28 (t, 2 H, $^3J_{H-H}$ = 8.0 Hz, H_4-Mebpy), 8.14 (d, 4 H, $^3J_{H-H}$ = 6.7 Hz, H_α-py), 7.89 (d, 4 H, $^3J_{H-H}$ = 6.8 Hz, H_β-py), 8.03−7.96 (m, 4 H, $H_{5,5'}$-Mebpy), 3.29 (s, 6 H, −C*H*$_3$). ^{13}C NMR (acetone-d_6): 197.4, 196.1, 192.7, 164.4, 163.5, 157.6, 157.3, 154.7, 153.9, 148.8, 148.6, 142.4, 142.2, 141.5, 130.4, 129.8, 127.5, 126.0, 123.3, 117.4, 117.3, 31.3. ES-MS: *m*/*z* = 1344.3 (calcd *m*/*z* = 1346.1 for $[M - PF_6^-]^+$). Anal. Calcd for $C_{45}H_{33}N_9O_8Re_2P_2F_{12}$: C, 36.27; H, 2.23; N, 8.46. Found: C, 35.95; H, 2.09; N, 8.70.

$[(4,4'\text{-}t\text{Bu}_2\text{bpy})\text{Re}(CO)_3]_2(\mu\text{-}2)(PF_6)_2$ (6). The same procedure for preparing **4** was employed to synthesize **6**. The purification was achieved by recrystallization from CH_2Cl_2/hexane to give the yellowish powder of **6**. Yield: 82%. IR ($\nu_{C\equiv O}$, CH_2Cl_2): 2033, 1930. ^{1}H NMR (300 MHz, CD_2Cl_2): 9.02 (d, 4 H, $^3J_{H-H}$ = 6.0 Hz, $H_{6,6'}$-Bu_2bpy), 8.96 (s, 2 H, −N*H*), 8.17 (d, 4 H, $^4J_{H-H}$ = 1.8 Hz, $H_{3,3'}$-Bu_2bpy), 8.10 (dd, 2 H, $^3J_{H-H}$ = 7.8 Hz, $^4J_{H-H}$ = 1.3 Hz, Ph-4,6), 8.03 (s, 1 H, Ph-2), 7.99 (d, 4 H, $^3J_{H-H}$ = 7.0 Hz, H_α-py), 7.76−7.72 (m, 8 H, $H_{5,5'}$-Bu_2bpy, H_β-py), 7.61 (t, 1 H, $^3J_{H-H}$ = 7.8 Hz, Ph-5), 1.45 (s, 36 H, −C*H*$_3$). ^{13}C NMR (CD_2Cl_2): 196.5, 191.9, 167.1, 166.5, 156.3, 153.3, 152.4, 148.9, 134.4, 133.9, 130.5,

(6) (a) Sun, S.-S. Lees, A. J. *Chem. Commun*. **2000**, 1687. (b) Sun, S.-S. Lees, A. J. *Coord. Chem. Rev*. **2002**, *230*, 171.
(7) (a) Sun, S.-S.; Zavilij, P.; Lees, A. J. *Acta Crystallogr*. **2001**, *E57*, m119. (b) Caspar, J. V.; Meyer, T. J. *J. Phys. Chem*. **1983**, *87*, 952.

126.8, 124.5, 121.7, 117.2, 36.6, 30.5. ES-MS: m/z = 1540.46 (calcd m/z = 1540.59 for $[M - PF_6^-]^+$) and m/z = 697.25 (calcd m/z = 697.81 for $[M - 2PF_6^-]^{2+}$). Anal. Calcd for $C_{60}H_{62}N_8O_8Re_2P_2F_{12}$: C, 42.76; H, 3.71; N, 6.65. Found: C, 42.28; H, 3.46; N, 6.19.

[(4,4′-*t*Bu$_2$bpy)Re(CO)$_3$]$_2$(μ-3)(PF$_6$)$_2$ (7). The same procedure for preparing **4** was employed to synthesize **7**. The purification was achieved by recrystallization from CH_2Cl_2/hexane to give the yellowish powder of **7**. Yield: 78%. IR ($\nu_{C\equiv O}$, CH_2Cl_2): 2033, 1927. ^{1}H NMR (300 MHz, $CDCl_3$): 9.10 (s, 2 H, −N*H*), 8.95 (d, 4 H, $^3J_{H-H}$ = 5.9 Hz, $H_{6,6'}$-Bu$_2$bpy), 8.23 (s, 4 H, $H_{3,3'}$-Bu$_2$bpy), 7.91 (d, 4 H, $^3J_{H-H}$ = 6.5 Hz, H_α-py), 7.71 (d, 4 H, $^3J_{H-H}$ = 5.7 Hz, $H_{5,5'}$-Bu$_2$bpy), 7.66 (d, 4 H, $^3J_{H-H}$ = 6.3 Hz, H_β-py), 7.49 (s, 4 H, ph), 1.42 (s, 36 H, −C*H*$_3$). ^{13}C NMR ($CDCl_3$): 196.1, 191.7, 166.7, 166.6, 155.9, 152.9, 151.8, 149.2, 136.6, 128.5, 126.4, 121.7, 117.2, 36.3, 30.4. ES-MS: m/z = 1540.49 (calcd m/z = 1540.59 for $[M - PF_6^-]^+$) and m/z = 697.76 (calcd m/z = 697.81 for $[M - 2PF_6^-]^{2+}$). Anal. Calcd for $C_{60}H_{62}N_8O_8Re_2P_2F_{12}$: C, 42.76; H, 3.71; N, 6.65. Found: C, 42.91; H, 3.66; N, 6.82.

(4,4′-*t*Bu$_2$bpy)Re(CO)$_3$(nicotinanilide)(PF$_6$) (8). The same procedure for preparing **4** was employed to synthesize **8**. Recrystallization from CH_2Cl_2/pentane afforded yellowish crystals of **8**. Yield: 79%. IR ($\nu_{C\equiv O}$, CH_2Cl_2): 2034, 1931. ^{1}H NMR (300 MHz, $CDCl_3$): 8.96 (d, 2 H, $^3J_{H-H}$ = 5.9 Hz, $H_{6,6'}$-Bu$_2$bpy), 8.34 (s, 1 H, −N*H*), 8.28 (s, 1 H, H_2-py), 8.22 (d, 2 H, $^4J_{H-H}$ = 1.7 Hz, $H_{3,3'}$-Bu$_2$bpy), 8.16 (d, 1 H, $^3J_{H-H}$ = 5.4 Hz, H_6-py), 8.02 (d, 1 H, $^3J_{H-H}$ = 7.9 Hz, H_4-py), 7.67 (d, 2 H, $^3J_{H-H}$ = 5.7 Hz, $^4J_{H-H}$ = 1.6 Hz, $H_{5,5'}$-Bu$_2$bpy), 7.55 (d, 2 H, $^3J_{H-H}$ = 7.6 Hz, H_o-ph), 7.31−7.25 (m, 3 H, H_5-py, H_m-ph), 7.08 (t, 1 H, $^3J_{H-H}$ = 7.3 Hz, H_p-ph), 1.37 (s, 18 H, −C*H*$_3$). ^{13}C NMR ($CDCl_3$): 195.9, 191.8, 166.6, 163.2, 156.3, 152.6, 151.9, 150.9, 138.2, 137.8, 135.4, 129.1, 126.7, 126.1, 125.0, 122.7, 120.6, 36.3, 30.1. ES-MS: m/z = 737.26 (calcd m/z = 736.87 for $[M - PF_6^-]^+$). Anal. Calcd for $C_{33}H_{34}N_4O_4RePF_6$: C, 44.95; H, 3.89; N, 6.35. Found: C, 45.16; H, 3.47; N, 6.77.

(4,4′-*t*Bu$_2$bpy)Re(CO)$_3$(4-NH$_2$py)(PF$_6$) (9). To a 100-mL flask containing (4,4′-*t*Bu$_2$bpy)Re(CO)$_3$(CH_3CN)(PF_6) (500 mg, 0.69 mmol) and 4-aminopyridine (4-NH_2py) (68 mg, 0.72 mmol) was added 30 mL of THF. The resulting mixture was refluxed for 16 h. Subsequently, the solution was cooled to room temperature and filtered. The filtrate was layered with 100 mL of hexane and allowed to stand for 2 days to afford yellowish microcrystals. Yield: 92%. IR ($\nu_{C\equiv O}$, CH_2Cl_2): 2030, 1925. ^{1}H NMR (300 MHz, acetone-d_6): 9.26 (d, 2 H, $^3J_{H-H}$ = 5.5 Hz, $H_{6,6'}$-Bu$_2$bpy), 8.76 (d, 2 H, $^4J_{H-H}$ = 1.5 Hz, $H_{3,3'}$-Bu$_2$bpy), 7.95 (d, 2 H, $^4J_{H-H}$ = 5.9 Hz, 1.5 Hz, $H_{5,5'}$-Bu$_2$bpy), 7.78 (d, 2 H, $^3J_{H-H}$ = 7.0 Hz, H_α-py), 6.49 (d, 2 H, $^3J_{H-H}$ = 7.1 Hz, H_β-py), 6.43 (bs, 2 H, −NH_2), 1.44 (s, 36 H, −C*H*$_3$). ^{13}C NMR (acetone-d_6): 197.4, 193.4, 167.0, 157.3, 156.9, 154.4, 152.1, 126.8, 123.1, 111.5, 36.8. ES-MS: m/z = 633.25 (calcd m/z = 632.76 for $[M - PF_6^-]^+$). Anal. Calcd for $C_{26}H_{30}N_4O_3RePF_6$: C, 40.15; H, 3.89; N, 7.20. Found: C, 40.58; H, 3.64; N, 7.22.

[(4,4′-*t*Bu$_2$bpy)Re(CO)$_3$]$_2$(μ-BPA)(PF$_6$)$_2$ (10). To a 100-mL flask containing (4,4′-*t*Bu$_2$bpy)Re(CO)$_3$(CH_3CN)(PF_6) (100 mg, 0.14 mmol) and 1,2-bis(4-pyridyl)ethane (BPA) (12 mg, 0.065 mmol) was added 30 mL of THF. The resulting mixture was refluxed for 16 h. Subsequently, the solution was cooled to room temperature and the solvent was removed under reduced pressure. The residue was dissolved in 20 mL of CH_2Cl_2 and filtered to remove any undissolved material. The filtrate was layered with 100 mL of hexane and allowed to stand for 2 days to afford yellowish microcrystals. Yield: 86%. IR ($\nu_{C\equiv O}$, CH_2Cl_2): 2033, 1929. ^{1}H NMR (300 MHz, acetone-d_6): 9.28 (d, 4 H, $^3J_{H-H}$ = 5.9 Hz, $H_{6,6'}$-Bu$_2$bpy), 8.72 (d, 4 H, $^4J_{H-H}$ = 1.7 Hz, $H_{3,3'}$-Bu$_2$bpy), 8.37 (d, 4 H, $^3J_{H-H}$ = 6.5 Hz, H_α-py), 7.95 (d, 4 H, $^3J_{H-H}$ = 5.9 Hz, $^4J_{H-H}$ = 1.9 Hz, $H_{5,5'}$-Bu$_2$bpy), 7.35 (d, 4 H, $^3J_{H-H}$ = 6.5 Hz, H_β-py), 2.90 (s, 4 H, −CH_2−), 1.42 (s, 72 H, −C*H*$_3$). ^{13}C NMR (acetone-d_6): 196.8, 192.9, 167.1, 156.9, 155.8, 154.5, 152.8, 127.7, 127.0, 123.1, 36.8, 34.9. ES-MS: m/z = 1406.54 (calcd m/z = 1406.50 for $[M - PF_6^-]^+$). Anal. Calcd for $C_{54}H_{60}N_6O_6Re_2P_2F_{12}$: C, 41.81; H, 3.90; N, 5.42. Found: C, 41.87; H, 3.79; N, 5.52.

Equipment and Procedures. NMR spectra were obtained using a Brucker AM 360 spectrometer or a Brucker AC 300 spectrometer. ^{1}H NMR spectra are reported in ppm relative to the proton resonance resulting from incomplete deuteration of the NMR solvent. Infrared spectra were measured on a Nicolet 20SXC Fourier transform infrared spectrophotometer. Mass spectrometry was provided by the Washington University Mass Spectrometry Resource. Elemental analyses were performed by Oneida Research Service, Whitesboro, New York. UV−vis spectra were obtained using a HP 8450A diode array spectrophotometer. Emission spectra were recorded in deoxygenated solvent solution at 293 K with an SLM 48000S lifetime fluorescence spectrophotometer equipped with a red-sensitive Hamamatsu R928 photomultiplier tube. The emission lifetimes were collected on a PRA system 300 time-correlated pulsed single-photon apparatus. The obtained lifetimes were fitted to a single-exponential decay in each case (PRA system software v.3.0) and found to be reproducible to within 5%. Detailed procedures for luminescence and lifetime experiments have been described in previous papers.[8]

Crystallography. Yellowish single crystals of complexes **8** and **9** suitable for X-ray diffraction studies were grown from slow diffusion of hexane into a concentrated complex solution in CH_2Cl_2. The crystals were measured on a Bruker Smart Apex CCD single-crystal diffractometer.[9a] Crystal structures were determined by the direct method and refined by a least-squares procedure using SHELXS97 and SHELXL97 crystallographic packages.[9b]

Determination of Association Constants (K_a) by Luminescent Spectrophotometric Titration. The binding studies were conducted in air-equilibrated CH_2Cl_2 solution. We found that the emission intensities were about 10% lower than those from deoxygenated CH_2Cl_2 solutions. However, the resultant I/I_0 ratio and fitted binding constants toward different anions did not change upon deaeration.

A receptor solution (2×10^{-6} M) was titrated by addition of aliquots of the anion solution (5×10^{-4}−1×10^{-3} M) prepared by a stock solution of the receptor. The observed emission intensities were then monitored as a function of the anion concentration. All of the titration curves were well fitted to 1:1 binding isotherms as shown below.

For a 1:1 receptor and anion binding system, the solution contains receptor (R), anion (A), and associated complex (RA). At the very low receptor concentration, and with the assumption that no excited-state association occurs, then the observed emission intensity can be expressed as eq 1.[10]

Nonlinear regression fitting of the data of I/I_0 versus [A] gives the association constant, K_a.

$$\frac{I}{I_0} = \frac{1 + (k_{11}/k_R)K_a[A]}{1 + K_a[A]}$$

(8) (a) Sun, S.-S.; Lees, A. J. *J. Am. Chem. Soc*. **2000**, *122*, 8956. (b) Wang, Z.; Lees, A. J. *Inorg. Chem*. **1993**, *32*, 1493.
(9) (a) *SMART and SAINT*; Bruker AXS Inc.: Madison, WI, 1999. (b) Sheldrick, G. M. *SHELXS97 and SHELXL97*; University of Göttingen: Göttingen, Germany, 1997.
(10) (a) Connors, K. A. *Binding Constant*; Wiley: New York 1987. (b) Novikov, E.; Stobiecka, A.; Boens, N. *J. Phys. Chem. A* **2000**, *104*, 5388.

Scheme 1

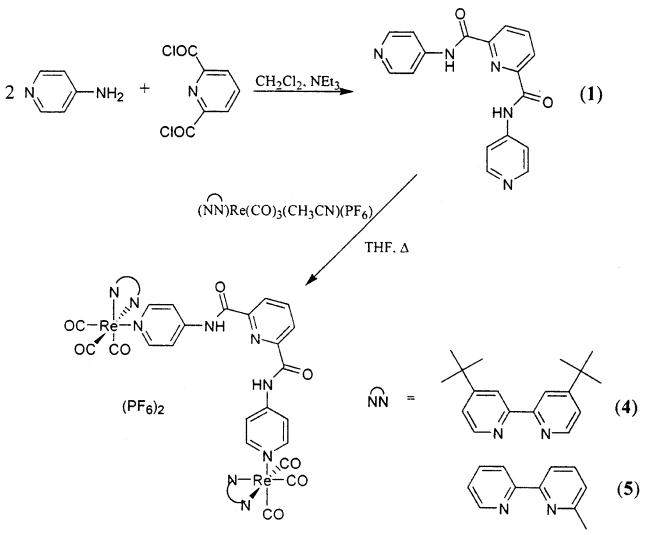

Scheme 2

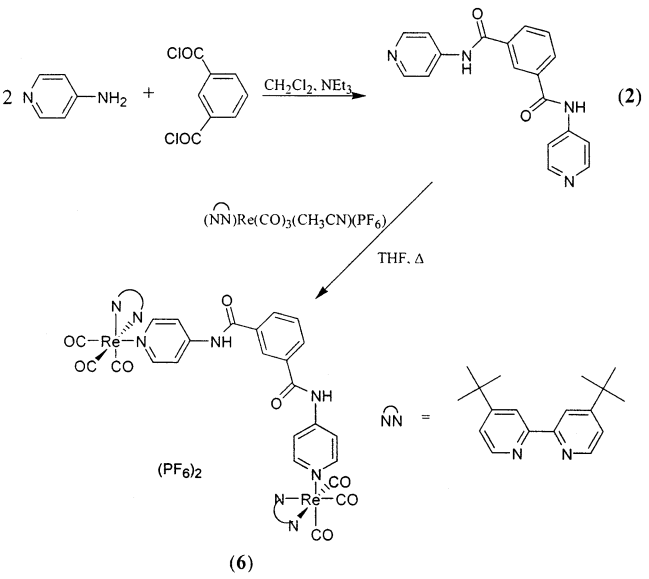

Results and Discussion

Synthesis and General Properties. The syntheses of ligand **1** and complexes **4** and **5** are shown in Scheme 1. The bridging ligand **1** was prepared in 56% yield from 2 equiv of 4-aminopyridine and 2,6-pyridinedicarbonyl dichloride. Ligand **1** exhibits very poor solubility in most common organic solvents, presumably because of its potential for intermolecular hydrogen-bonding formation via the amide protons. Subsequent reaction of **1** and 2 equiv of $(CH_3CN)(4,4'\text{-}t\text{Bu}_2\text{bpy})\text{Re(CO)}_3(PF_6)$ or $(CH_3CN)(6\text{-Mebpy})\text{Re(CO)}_3(PF_6)$ in refluxing THF, followed by recrystallization from CH_2Cl_2/pentane (**4**) or CH_3CN/ether (**5**), afforded bright yellow crystalline solids **4** and **5** in 81% and 88% yield, respectively.

The syntheses of ligand **2** and complex **6** are shown in Scheme 2. The bridging ligand **2** was prepared in 62% yield from 2 equiv of 4-aminopyridine and isophthaloyl dichloride. Due to the extremely low solubility of ligand **2** in THF, the subsequent metal-complexation process needed to reflux for 3 days to ensure the completion of the reaction. The yellowish powder of complex **6** was isolated after recrystallization from CH_2Cl_2/hexane in 82% yield.

Scheme 3

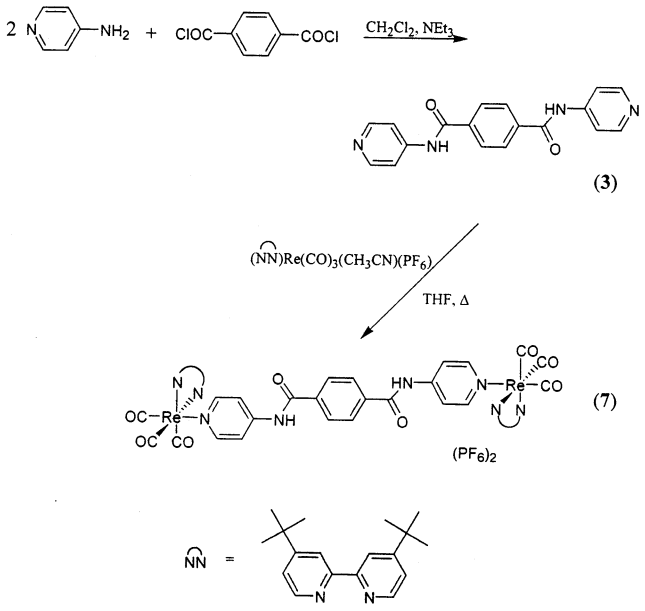

Similarly, the syntheses of ligand **3** and complex **7** are shown in Scheme 3. Ligand **3** was synthesized in 62% yield from 2 equiv of 4-aminopyridine and terephthaloyl chloride. It has been found the reaction can be carried out only with a relative small amount of starting materials and with a large quantity of solvent to ensure the solubility of the condensation products. Subsequent reaction of **3** and 2 equiv of $(CH_3CN)(4,4'\text{-}t\text{Bu}_2\text{bpy})\text{Re(CO)}_3(PF_6)$ in refluxing THF, followed by recrystallization from CH_2Cl_2/hexane, afforded a bright yellow crystalline solid **7** in 78% yield.

Complexes **8**−**10** were synthesized from reaction of $(CH_3CN)(4,4'\text{-}t\text{Bu}_2\text{bpy})\text{Re(CO)}_3(PF_6)$ and nicotinanilide, 4-NH_2-py, or 0.5 equiv of BPA in refluxing THF, as shown in Scheme 4, and purified by recrystallization from CH_2Cl_2/hexane solution, which afforded pale yellow microcrystals in 76% yield for **8**, 92% yield for **9**, and 86% yield for **10**. The identity and purity of all new compounds have been established by NMR, mass spectrometry, and elemental analysis.

The N−H protons of complex **4** exhibit a chemical shift of 10.59 ppm in $CDCl_3$. The highly downfield chemical shift in a non-hydrogen bond donating solvent indicates the presence of strong intramolecular hydrogen bonding between the N−H protons and the nitrogen of the central pyridine. This results in ligand **1** having an approximate right angle geometry,[11] and the converged structure of complex **4** renders

(11) (a) Bisson, A. P.; Lynch, V. M.; Monahan M.-K. C.; Anslyn, E. V. *Angew. Chem., Int. Ed. Engl.* **1997**, *36*, 2340. (b) Hunter C. A.; Sarson, L. D. *Angew. Chem., Int. Ed. Engl.* **1994**, *33*, 2313. (c) Jeong, K.-S.; Cho, Y. L.; Song, J. U.; Chang, H.-Y.; Choi, M.-G. *J. Am. Chem. Soc.* **1998**, *120*, 10982. (d) Hunter, C. A.; Low, C. M. R.; Packer, M. J.; Spey, S. E.; Vinter, J. G.; Vysotsky, M. O.; Zonta, C. *Angew. Chem., Int. Ed.* **2001**, *40*, 2678. (e) Huang, B.; Parquette, J. R. *Org. Lett.* **2000**, *2*, 239. (f) Hamuro, Y.; Geib, S. J.; Hamilton, A. D. *Angew. Chem., Int. Ed. Engl.* **1994**, *33*, 446.

Scheme 4

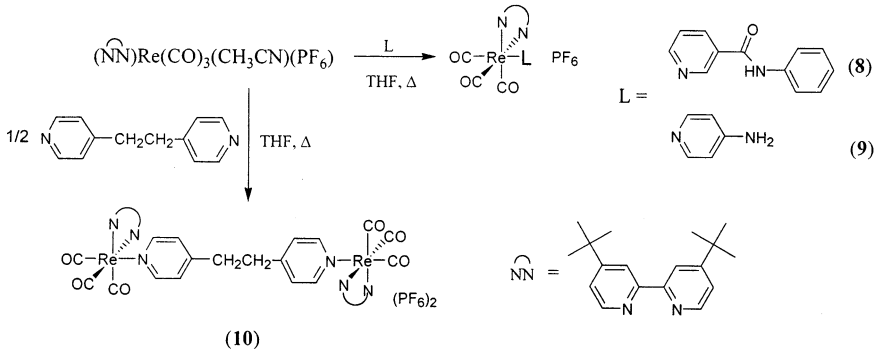

Table 1. Crystal Data for **8**·1.5CH_2Cl_2 and **9**[a]

	8·1.5CH_2Cl_2	**9**
formula	$C_{34.5}H_{37}Cl_3F_6N_{16}O_{16}PRe$	$C_{26}H_{30}F_6N_4O_3PRe$
cryst system	monoclinic	orthorhombic
space group	$P2_1/n$	Pnma
a, Å	12.497(2)	10.7397(5)
b, Å	11.340(2)	16.6829(9)
c, Å	29.672(6)	18.0705(10)
α, deg	90	90
β, deg	92.819(4)	90
γ, deg	90	90
V, Å^3	4199.8(14)	3237.7(3)
Z	4	4
fw	1009	778
F_{000}, e	1996	1528
D_{calc}, g cm^{-3}	1.596	1.595
μ, mm^{-1}	3.189	3.869
crystal color	light yellow	yellow
dimens, mm	0.31 × 0.20 × 0.14	0.45 × 0.10 × 0.08
abs method	multiscan, SAINT	multiscan, SADBAS
min/max transm	0.43, 0.64	0.49, 0.73
decay corr, %	10	
tot. reflcns	20 097	28 609
unique reflcns	6672	5066
obsd reflcs	3458	3112
refined params	523	236
coverage, %	99.9	99.4
$2\theta_{max}$	48.2	61.2
R_{eq}	0.0801	0.0630
R_{sig}	0.1274	0.0488
R_w	0.1442	0.0930
R_{F^2} ($I > 2\sigma(I)$)	0.0596	0.0381

[a] All experimental diffraction data were collected at room temperature on a Bruker single-crystal diffractometer with SmartApex CCD detector, Mo Kα radiation, and *ω*-scans with 0.3° steps. Absorption correction was done using a multiscan method. Crystal structures were solved by the direct methods and refined using *SHELX* software. Ellipsoid drawings were created using an ORTEP program.

it as an effective anion receptor through hydrogen bonding. Similarly, the highly downfield chemical shift (11.06 ppm) of the amide protons is also observed in complex **5**. It should be pointed out, however, that the more downfield shifting of the amide protons in complex **5** compared to the ones in complex **4** could be simply due to the presence of trace amount of water in the deuterated acetone, not really indicating a stronger hydrogen bonding in complex **5** than in complex **4**. In the case of complex **8**, the *meta* connection between the amide group and nitrogen in the pyridine results in no intramolecular hydrogen bonding and it is obvious that the chemical shift of the amide proton appears at the normal position, ca. 8.34 ppm. In the cases of complexes **6** and **7**, there is no chance to form intramolecular hydrogen bonding but there may be intermolecular hydrogen bonding between the amide protons and the carbonyl groups. This idea is

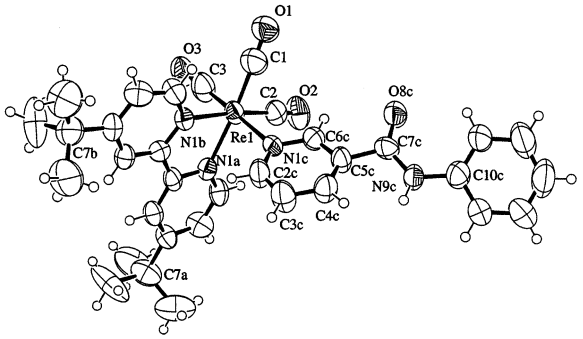

Figure 1. ORTEP drawing of crystal **8** with displacement ellipsoids at the 50% probability level.

Table 2. Selected Bond Distances (Å) of **8**·1.5CH_2Cl_2

Re1−C3	1.852(13)	Re1C1	1.895(13)	Re1C2	1.947(12)
Re1−N1a	2.179(8)	Re1N1b	2.180(8)	Re1N1c	2.224(8)
C1−O1	1.168(13)	C2−O2	1.127(12)	C3−O3	1.185(13)
N1a−C2a	1.354(13)	N1a−C6a	1.379(12)	C2a−C3a	1.351(14)
C3a−C4a	1.373(14)	C4a−C5a	1.373(14)	C4a−C7a	1.500(13)
C5a−C6a	1.387(13)	C6a−C6b	1.472(14)	C7a−C12a	1.554(10)
C7a−C8a	1.557(10)	C7a−C9a	1.558(10)	C7a−C11a	1.560(11)
C7a−C13a	1.563(11)	C7a−C10a	1.563(10)	N1b−C2b	1.321(13)
N1b−C6b	1.354(11)	C2b−C3b	1.369(15)	C3b−C4b	1.375(14)
C4b−C5b	1.400(14)	C4b−C7b	1.554(15)	C5b−C6b	1.362(13)
C7b−C10b	1.504(17)	C7b−C9b	1.544(18)	C7b−C8b	1.574(17)
N1c−C2c	1.308(12)	N1c−C6c	1.364(11)	C2c−C3c	1.360(14)
C3c−C4c	1.361(14)	C4c−C5c	1.350(13)	C5c−C6c	1.383(13)
C5c−C7c	1.515(14)	C7c−O8c	1.217(11)	C7c−N9c	1.311(12)
N9c−C10c	1.416(13)	C10c−C15c	1.372(15)	C10c−C11c	1.370(15)
C11c−C12c	1.411(17)	C12c−C13c	1.384(19)	C13c−C14c	1.315(18)
C14c−C15c	1.396(18)				

partially supported by the slightly downfield shifting of the amide protons at 8.96 and 9.10 ppm for complexes **6** and **7**, respectively. Complexes **9** and **10** were also synthesized to serve as model compounds. Complex **10** is employed to assess the position of MLCT band, while complex **9** is expected to form the weakest hydrogen bonding, if there is any, among all six complexes (**4**−**9**) studied in this paper.

Crystal Structure Analysis. Yellowish single crystals of complexes **8** and **9** suitable for X-ray diffraction studies were grown from slow diffusion of hexane into a concentrated complex solution in CH_2Cl_2. The molecular structures of **8**·1.5CH_2Cl_2 and **9** were established. The crystal data are collected in Table 1.

Structure 8·1.5CH_2Cl_2. An ORTEP drawing of complex **8** is shown in Figure 1. Selected bond distances, bond angles, and torsion angles are collected in Tables 2−4, respectively. The rhenium atom resides in an approximately octahedral

Table 3. Selected Bond Angles (deg) of **8**·1.5CH_2Cl_2

C3−Re1−C1	90.0(6)	C3−Re1−C2	88.7(5)
C1−Re1-C2	87.2(5)	C3−Re1−N1a	90.6(4)
C1−Re1−N1a	173.0(5)	C2−Re1−N1a	99.8(4)
C3−Re1−N1b	91.9(4)	C1−Re1−N1b	98.9(5)
C2−Re1−N1b	173.9(4)	N1a−Re1−N1b	74.1(3)
C3−Re1−N1c	178.4(4)	C1−Re1−N1c	91.6(4)
C2−Re1−N1c	91.6(4)	N1a−Re1−N1c	87.8(3)
N1b−Re1−N1c	87.6(3)	O1−C1−Re1	177.4(12)
O2−C2−Re1	175.8(10)	O3−C3−Re1	177.3(12)

Table 4. Torsion Angles (deg) of **8**·1.5CH_2Cl_2

N1a	C6a	C6b	N1b	0.5(12)
C3b	C4b	C7b	C10b	−11.0(17)
C3b	C4b	C7b	C8b	−130.9(13)
C3b	C4b	C7b	C9b	108.5(14)
C3a	C4a	C7a	C10a	53.6(14)
C3a	C4a	C7a	C8a	−64.6(13)
C3a	C4a	C7a	C9a	175.0(12)
C3a	C4a	C7a	C11a	−135.8(16)
C3a	C4a	C7a	C12a	−14.2(19)
C3a	C4a	C7a	C13a	107.8(16)
C4c	C5c	C7c	O8c	−154.7(12)
C4c	C5c	C7c	N9c	27.8(18)
C5c	C7c	N9c	C10c	175.7(11)
C7c	N9c	C10c	C11c	26.6(19)

environment with the facial disposition for the three carbonyl groups. The Py−CONH−Ph moiety and one CO group are opposite while 4,4′-*t*Bu_2bpy and two other CO groups are planar. The carbonyl Re−C bond distances range from 1.852 to 1.947 Å. The Re−N bond distances range from 2.179 to 2.224 Å. The Re−C−O linkage (175.8(10)−177.4(12)°) does not deviate significantly from linearity. All determined carbonyl Re−C and Re−N bond distances appear to be normal.[7a,12] The Py−CONH−Ph moiety is not flat and it is tilted around the C5c−C6c and N9c−C10c bonds at about 25°, while the CONH group remains practically flat along with attached C5c and C10c. One of two methyl groups in 4,4′-*t*Bu_2bpy is disordered in two orientations at about 60° to each other. It is noticeable that there are large thermal motions of PF_6 and two identifiable CH_2Cl_2 molecules, one of which is disordered into two positions near the center of symmetry.

Structure 9. An ORTEP drawing of complex **9** is shown in Figure 2. Selected bond distances and bond angles are collected in Tables 5 and 6, respectively. The complex lies on the mirror plane in such a way that $PyNH_2$ and the trans CO group are in the plane, while the 4,4′-*t*Bu_2bpy moiety is perpendicular to this plane. The PF_6 anion is disordered in two positions near the mirror plane. The Re−C bond distances range from 1.907 to 1.912 Å. The Re−N bond distances range from 2.164 to 2.224 Å. The Re−C−O linkage (178.1(4)−179.7(4)°) does not deviate significantly from linearity.

Photophysical Properties. The absorption and emission spectral data along with lifetimes and emission quantum yields in deoxygenated CH_2Cl_2 at 293 K are summarized in Table 7. In general, the absorption spectra of all the

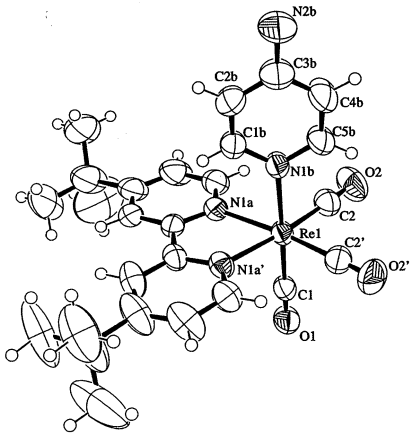

Figure 2. ORTEP drawing of crystal **9** with displacement ellipsoids at the 50% probability level.

Table 5. Selected Bond Distances (Å) of **9**

Re1−C1	1.907(6)	Re1−C2	1.916(5)	Re1−C2′	1.916(5)
Re1−N1a	2.164(3)	Re1−N1a	2.164(3)	Re1−N1b	2.224(5)
C1−O1	1.139(6)	C2−O2	1.149(5)	N1b−C5b	1.349(7)
N1b−C1b	1.355(7)	C1b−C2b	1.346(9)	C2b−C3b	1.396(11)
C3b−N2b	1.358(8)	C3b−C4b	1.367(10)	C4b−C5b	1.372(9)

Table 6. Selected Bond Angles (deg) of **9**

C1−Re1−C2	88.44(18)	C1−Re1−C2	88.44(17)
C2−Re1−C2	89.0(3)	C1−Re1−N1a	91.58(15)
C2−Re1−N1a′	172.71(16)	C2−Re1−N1a	98.27(17)
C1−Re1−N1a	91.58(15)	N1a−Re1−N1a′	74.44(17)
C1−Re1−N1b	178.84(19)	C2−Re1−N1b	92.38(16)
N1a−Re1−N1b	87.50(13)	O1−C1−Re1	179.7(5)
O2−C2−Re1	178.1(4)		

complexes exhibit a series of strong absorption bands below 335 nm. These bands are assigned to ligand-based $\pi-\pi^*$ transitions. The absorption spectra of complexes **4** and **10** as well as their difference spectrum are displayed in Figure 3. The low-energy shoulder around 380 nm in complex **4** disappears in the difference spectrum, and this confirms that the lowest excited state is a Re (dπ) to 4,4′-*t*Bu_2bpy (π^*) charge-transfer band. The low-energy features around 370 nm in complexes **6**−**8** are also assigned to Re (dπ) to 4,4′-*t*Bu_2bpy (π^*) charge-transfer bands. This assignment is also supported by the appearance of an absorption band at 368 nm in complex **9** where the only low-energy transition is the Re (dπ) to 4,4′-*t*Bu_2bpy (π^*) charge-transfer band. Similarly, the shoulder appearing at 368 nm in complex **5** is assigned to a Re (dπ) to 6-Mebpy (π^*) charge-transfer band.

All six complexes exhibit fairly strong luminescence in CH_2Cl_2 solution at room temperature. The structureless spectral profiles and submicrosecond lifetimes indicate that the emissions of all six complexes originate from the ^{3}MLCT excited states. The calculated k_r values are also very typical for triplet MLCT emissions, ca. 1×10^5 s^{-1}.[13] The photophysical parameters of complexes **4**, **6**, and **7** are virtually the same. This is not unexpected given that the lowest excited states in both these complexes are Re (dπ) to 4,4′-*t*Bu_2bpy (π^*) CT states and the bridging ligands are structurally similar amide−pyridines.

(12) (a) Chen, P. C.; Curry, M.; Meyer, T. J. *Inorg. Chem.* **1989**, *28*, 2271. (b) Xue, W.-M.; Goswami, N.; Eichhorn, D. M.; Orizondo, P. L.; Rillema, D. P. *Inorg. Chem.* **2000**, *39*, 4460. (c) Lin, J. T.; Sun, S.-S.; Wu, J. J.; Liaw, Y. C.; Lin, K. J. *J. Organomet. Chem.* **1996**, *517*, 217.

(13) Baba, A. I.; Shaw, J. R.; Simon, J. A.; Thummel, R. P.; Schmehl, R. H. *Coord. Chem. Rev.* **1998**, *171*, 43.

Table 7. Absorption and Emission Spectral Data and Calculated Photophysical Parameters of Complexes **4**−**10** in CH_2Cl_2 at 293 K

	absorption	emission[a]				
complexes	λ_{max}, nm ($10^{-3}\epsilon$, M^{-1} cm^{-1})	λ_{em}, nm	Φ_{em}	τ, μs	$10^{-5}k_r$, s^{-1}	10^{-6} k_{nr}
4	254 (63.6), 281 (61.5), 380 (sh, 7.70)	536	0.20	0.48	4.2	1.7
5	252 (45.6), 300 (47.6), 324 (sh, 35.9), 368 (6.02)	544	0.083	0.38	2.2	2.4
6	255 (50.1), 285 (53.0), 315 (sh, 33.6), 362 (7.84)	538	0.16	0.62	2.6	1.3
7	255 (52.7), 288 (56.4), 303 (sh, 54.5), 376 (sh, 8.03)	538	0.22	0.54	4.1	1.4
8	250 (35.2), 274 (34.7), 300 (sh, 25.6), 315 (22.1), 373 (sh, 5.11)	524	0.39	1.10	3.5	0.56
9	270 (30.6), 316 (sh, 9.82), 368 (4.09)	552	0.042	0.21	2.0	4.6
10	254 (40.9), 271 (41.6), 303 (sh, 28.1), 315 (24.8), 348 (sh, 9.42)	532	0.27	0.59	4.6	1.2

[a] λ_{ex} = 360 nm.

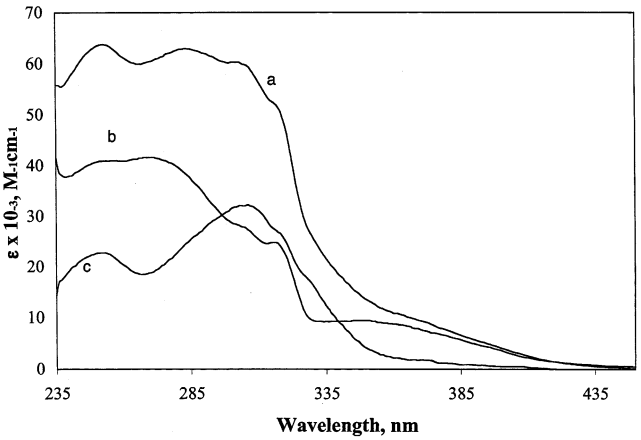

Figure 3. Absorption spectra of complexes **4** (curve a), **10** (curve b), and the difference spectrum between complexes **4** and **10** (curve c) in CH_2Cl_2 at 293 K.

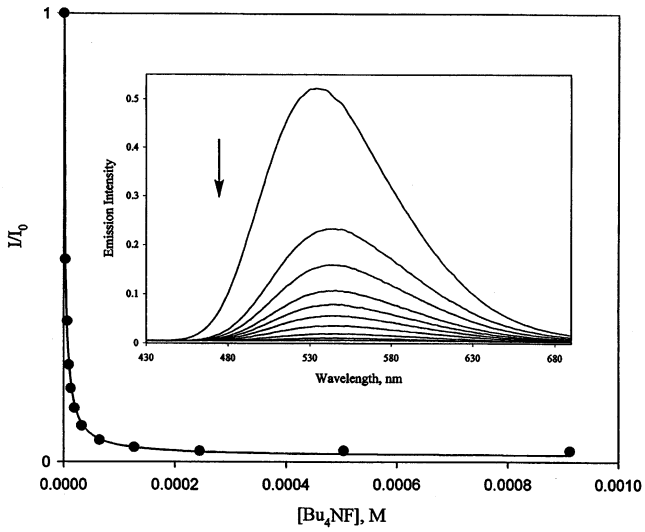

Figure 4. Titration curve of the addition of F^- anion (as tetrabutylammonium salt) monitored by luminescence spectroscopy. The inset showed the change of the emission intensity of complex **4** in CH_2Cl_2 solution upon addition of F^- anion. The emission spectra of the two lowest anion concentrations were not included for clarity. The excitation wavelength is 360 nm.

Anion Binding Studied by Luminescence Spectroscopy. The anionic sensory system studied here comprises an amide−pyridine moiety, which provides the anion binding site through amide−anion hydrogen bonding and a signaling unit which is (4,4′-*t*Bu_2bpy)Re(CO)$_3$. The positive-charged character of the (4,4′-*t*Bu_2bpy)Re(CO)$_3$ moiety is also expected to provide an additional electron-withdrawing effect on the amide binding site.[14] Addition of different halides or inorganic polyatomic anions (as tetrabutylammonium salts) into a 2×10^{-6} M solution of complexes **4**−**9** was observed to cause different degrees of quenching of the luminescence intensities. Except for complex **9**, the N−H protons in ^{1}H NMR spectra all showed significant downfield shifts (>1.5 ppm), indicating the strong hydrogen-bonding formation between the amide protons of the complexes and the anions. In the case of complex **9**, there is no significant decrease in the emission intensity when the complex is exposed to anions. The titration curves were observed to fit well to a 1:1 binding isotherm, and the binding stoichiometry was further confirmed by Job plots.[10a]

Figure 4 shows a typical 1:1 titration curve for the luminescence intensity upon addition of F^- to a CH_2Cl_2 solution of complex **4**. Concomitant with the quenching, the luminescence maximum red-shifts approximately 6−10 nm in each case. The lowest-energy band (^{1}MLCT) in the absorption spectrum also red-shifts 10−30 nm in each case along with the decrease of the $\pi-\pi^*$ band at 281 nm, and a new band developed around 347 nm (with a shoulder around 436 nm) upon addition of anion into the receptor solution (see Figure 5).

However, in the case of I^-, there was no apparent change in the absorption spectrum. The red shift of the absorption and emission positions, as well as the quenching of the emission intensities upon addition of anions, is not obvious but is likely due to a switching of the lowest excited state from 4,4′-*t*Bu_2bpy-based ^{3}MLCT state to amide−pyridine-based ^{3}MLCT state through hydrogen-bonding formation, thereby enhancing nonradiative decay. This conclusion is partially supported by low-level extended Hückel calculations where the LUMO changes from π^* orbital localized on 4,4′-*t*Bu_2bpy to the π^* orbital localized on the amide−pyridine ligand upon formation of hydrogen bonding between the anion and amide protons. Scheme 5 depicts possible qualitative excited-state diagrams representing the respective charge-transfer energy levels before and after anion binding. Similar red shifts on the emission spectra and quenching of the emission intensities upon anion binding were also observed in Ru(II)−polypyridine-based sensing systems.[5b,15] Further experiments (emission lifetimes, NMR titration studies, and

(14) Chao, I.; Hwang, T.-S. *Angew. Chem., Int. Ed.* **2001**, *40*, 2775.

(15) Excited-state reordering by protonation or deprotonation of ligands in metal complexes is a known phenomenon. See for example: Coates, C. G.; Keyes, T. E.; McGarvey, J. J.; Hughes, H. P.; Vos, J. G.; Jayaweera, P. M. *Coord. Chem. Rev.* **1998**, *171*, 323.

Scheme 5

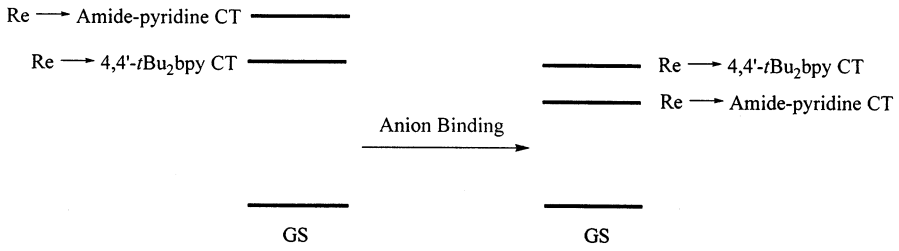

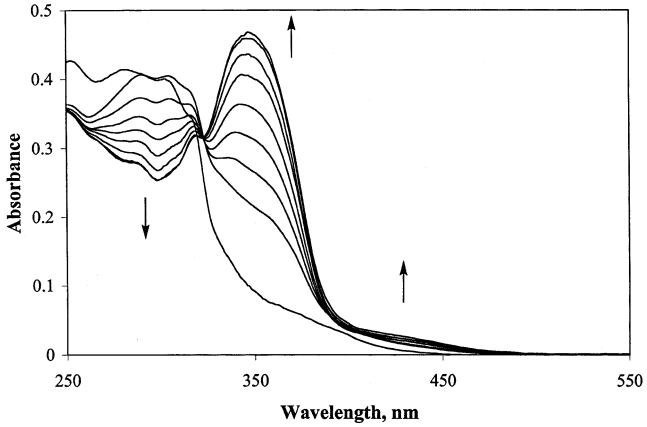

Figure 5. Changes in the absorption spectra of complex **4** (6.7×10^{-6} M) in CH_2Cl_2 solution upon addition of F^- anion (as tetrabutylammonium salt). The concentrations of F^- anion are 0, 4.0×10^{-5}, 5.9×10^{-5}, 9.8×10^{-5}, 1.9×10^{-4}, 3.7×10^{-4}, 6.9×10^{-4}, 1.3×10^{-3}, and 2.2×10^{-3} M, respectively.

Table 8. Association Constants K_a of Complexes **4**−**8** toward Different Anions Determined by Luminescence Titration in CH_2Cl_2 at 298 K

	$10^{-4}K_a$, M^{-1}				
anions	**4**	**5**	**6**	**7**	**8**
CN^-	88	14	1.5	2.3	1.5
F^-	38	2.8	2.5	6.0	1.1
Cl^-	4.0	1.6	0.41	0.75	0.33
Br^-	3.9	2.4	0.38	0.44	0.22
I^-	15[a]	2.7[a]	5.7[a]	1.1[a]	1.60[a]
OAc^-	3.4	1.4	0.71	0.73	1.6
$H_2PO_4^-$	0.015	0.010	18	5.5	1.6
NO_3^-	6.3×10^{-3}	5.9×10^{-3}	0.47	0.52	0.34
ClO_4^-	8.4×10^{-4}	7.4×10^{-4}	4.5×10^{-3}	2.0×10^{-3}	3.1×10^{-3}

[a] Possibly involves an excited-state association process. See text for details.

electrochemical measurements) designed to elucidate the identity of the excited states and quenching mechanism upon anion binding are currently underway. At this stage, it appears that a dynamic quenching mechanism does not occur in this system given the fact that there was no apparent quenching between complex **10** and the various anions studied. Another possible explanation for the observed emission quenching behavior is anion-enhanced reductive quenching of the MLCT excited state; this would also be expected to lower the energy of the Re(I) to pyridine−amide ligand charge-transfer excited state.

Table 8 summarizes the binding constants measured for complexes **4**−**8** toward different anions. Clearly, complexes **4** and **5** show strong binding affinity toward halides, cyanide, or acetate anions, only moderate binding affinity toward dihydrogen phosphate, and very weak binding affinity to nitrate or perchlorate anions. The overall order determined

Scheme 6

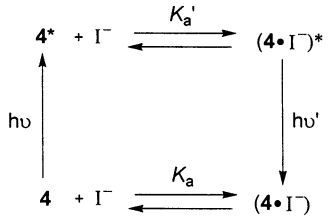

for binding affinity is the following: $CN^- > F^- > I^- > Cl^- \sim Br^- \sim OAc^- \gg H_2PO_4^- > NO_3^- > ClO_4^-$. This finding is significant as it is unusual for charged receptors to exhibit such outstanding selectivity for anion species.[11,16] In fact, the combination of interactions involving electrostatic forces, hydrogen-bonding strength, hydration energy, and steric effects all apparently influence the binding affinities toward anions in complexes **4** and **5**. Importantly, the sensitivities of complexes **4** and **5** are so high that the emission intensity can be effectively quenched by as much as 10% even in the presence of only 10^{-8} M cyanide or fluoride anions.

We are also surprised that I^- has higher association constant than both the Cl^- and Br^- anions. Given the fact that there was no apparent change in the absorption spectrum upon addition of I^- to the receptor solution (vide infra), the efficient emission quenching is likely due to the involvement of an excited-state association process (see Scheme 6).

To account for the unusual selectivity observed in complexes **4** and **5**, several structurally similar complexes were also synthesized and their anion binding studies were conducted under the same experimental conditions. Although the general trend of sensitivity still holds in complexes **6**−**8**, the selectivity toward different anions is greatly reduced. Except for ClO_4^-, which is expected to form the weakest hydrogen bond, all other anions studied in this research exhibit similar binding affinities within 2 orders of magnitude. The similar association constants of complexes **6** and **7** toward anions indicate that the two amide groups in complex **6** are arranged in an anti fashion. The intramolecular hydrogen-bonding capability of ligand **1,** which forces a cleft conformation, seems to be the key to its metal complexes being efficient as an anionic sensory system.

Conclusion

The design of highly sensitive and selective anion receptors is an emerging area in development of sensory systems.

(16) (a) Snowden, T. S.; Bisson, A. P.; Anslyn, E. V. *J. Am. Chem. Soc.* **1999**, *121*, 6324. (b) Kavallieratos, K.; de Gala, S. R.; Austin, D. J.; Crabtree, R. H. *J. Am. Chem. Soc.* **1997**, *119*, 2325.

Complexes **4** and **5** represent a simple and easy to prepare luminescent anion sensory system. These molecules display an outstanding selectivity for a variety of biologically and environmentally important anions. The strong binding affinity and high selectivity of both complexes for certain anions also may make them promising candidates for many other different applications besides sensors, such as homogeneous catalysis and membrane transport.

Acknowledgment. We are grateful to the Division of Chemical Sciences, Office of Basic Energy Sciences, Office of Science, U.S. Department of Energy (Grant DE-FG02-89ER14039), for support of this research. We also thank Mr. Shane Stephens-Romero for help synthesizing ligand **3**. Mass spectrometry was provided by the Washington University Mass Spectrometry Resource, an NIH Research Resource (Grant No. P41RR00954).

Supporting Information Available: Cystallographic files in CIF format. This material is available free of charge via the Internet at http://pubs.acs.org.

IC0206589